Random and correlated roughening in slow fracture by damage nucleation

Ido Ben-Dayan, Eran Bouchbinder, and Itamar Procaccia
Department of Chemical Physics, The Weizmann Institute of Science, Rehovot 76100, Israel
(Received 23 March 2006; published 4 October 2006)

We address the role of the nature of material disorder in determining the roughness of cracks, which grow by damage nucleation and coalescence ahead of the crack tip. We highlight the role of quenched and annealed disorders in relation to the length scales d and ξ_c associated with the disorder and the damage nucleation, respectively. In two related models, one with quenched disorder in which $d \simeq \xi_c$, the other with annealed disorder in which $d \ll \xi_c$, we find qualitatively different roughening properties for the resulting cracks in two dimensions. The first model results in random cracks with an asymptotic roughening exponent $\zeta \approx 0.5$. The second model shows correlated roughening with $\zeta \approx 0.66$. The reasons for the qualitative difference are rationalized and explained.

DOI: 10.1103/PhysRevE.74.046102 PACS number(s): 62.20.Mk, 81.40.Np

I. INTRODUCTION

When cracks develop slowly via the nucleation of damage ahead of the tip, the crack surfaces left behind appear to be rough. A question of great interest is, what is the scaling exponent that characterizes the roughening of such surfaces and how can one relate the value of the exponent to the physical phenomena that govern the crack propagation? For crack surfaces in 2+1 dimensions the anisotropy of the fracture experiment results in a number of scaling exponents, making the attainment of a satisfactory theory quite difficult [1]. On the other hand, for cracks in quasi-two-dimensional samples, where the resulting surfaces are 1+1-dimensional graphs (rupture lines), the issues are clear at least in the sense that there exists one well-defined scaling exponent. This is conveniently defined by measuring $y(x)$ where y is the height of the graph above the Euclidean coordinate x that defines the crack direction and then defining some measure of the height fluctuations; for example,

$$h(r) \equiv \langle \max\{y(\tilde{x})\}_{x<\tilde{x}<x+r} - \min\{y(\tilde{x})\}_{x<\tilde{x}<x+r} \rangle_x. \quad (1)$$

For self-affine graphs the scaling exponent ζ is defined via the scaling relation

$$h(r) \sim r^{\zeta}. \quad (2)$$

It is well known that random graphs are consistent with $\zeta = 0.5$, whereas positively (negatively) correlated graphs are characterized by $\zeta > 0.5$ ($\zeta < 0.5$). Experiments on two-dimensional samples tend to report scaling exponents in the range $\zeta \approx 0.65 \pm 0.04$ [2–4], indicating the existence of positive correlations between successive crack segments.

In recent work a model was proposed in 1+1 dimensions for such slow crack propagation via damage nucleation and coalescence ahead of the crack tip [5,6]. A crucial aspect of this model is the existence of a typical length scale ξ_c ahead of the crack tip where damage nucleation can take place [7]. A physical picture that might support such a scenario (though definitely not a unique one) is that a small plastic zone of linear dimension ξ_c forms around the crack tip and the relevant damage units involved in the process are plastic voids. The idea is that since plastic deformation is typically associated with a limiting stress level (denoted the "yield stress") σ_Y, the purely linear elastic divergent stresses are cut off such that they cannot reach a critical level required for the nucleation of voids *at the crack tip*. It is claimed that such critical levels of stress can be attained approximately near the outer boundary of the plastic zone, i.e., the elastic-plastic boundary. Whenever a void is nucleated in this region, it evolves and eventually coalesces with the current crack tip to form a new crack configuration. The crack then evolves by successive applications of such nucleation and coalescence events. References [5,6] demonstrated that the rupture lines generated by this model are self-affine rough graphs with a *correlated* scaling exponent $\zeta \approx 0.66$. Not only the value of the roughness exponent is found to be significantly above the random-walk exponent $\zeta = 0.5$, it also appears close to the measured one [2–4]. The aim of this paper is to gain a deeper understanding of the origin of this result.

An essential question asked in the context of any such fracture growth model is how to represent and incorporate the effect of material disorder. This issue is important since it asks how small-scale features affect large-scale properties, for example, the power-law scaling of Eq. (2) that indicates a lack of characteristic length scale. To our knowledge there had been no systematic study of the role of the nature of material disorder in determining the roughness of cracks in 1+1 dimensions. Our aim here is to shed some light on this issue by demonstrating that different views of material disorder and the associated length scales have a qualitative effect on the scaling properties of rupture lines. To this aim we elaborate on the type of material disorder adopted in the model described briefly above (referred to below as model A) and present a new model (referred to below as model B) that incorporates a different picture of material disorder. In model B the disorder is quenched, and the stochasticity associated with the material heterogeneities is fixed *a priori* in space and time. In model A the disorder is "annealed" in the sense that the stochasticity depends on the actual state of the system at each time. Whenever the disorder has some spatial characteristic scale we denote it by d and call it the "disorder length" that should be compared to the previously introduced length ξ_c. Thus model A is characterized by annealed disorder and $d \ll \xi_c$, while model B is characterized by quenched disorder and $d \simeq \xi_c$. One of the points of this paper is that this change in material disorder in model B is sufficient to de-

stroy the positive correlations between successive crack segments observed in model *A*, changing the universality class of the model and ending up with a random graph with an asymptotic scaling exponent $\zeta \approx 0.5$.

In Sec. II we present in more detail model *A* and recall its results, elaborating on the way in which material disorder is incorporated into the model. We then explain the modifications leading to model *B*. In Sec. III we present the new results for model *B*, compare them with model *A*, and clarify the origin of the qualitative differences between them. Section IV offers a summary and some concluding remarks.

II. CRACK PROPAGATION BY DAMAGE NUCLEATION AND COALESCENCE

A. A nonperturbative calculation of the linear-elastic stress fields

The mathematical difficulty in developing a theory for the morphology of fracture surfaces is the necessity of calculating the linear-elastic stress fields for highly nonregular crack paths. Typically, the stress conditions near the crack tip depend *nonlinearly* on the crack path $y(x)$. Formally, one has to solve the bi-Laplace equation for the Airy stress potential $\chi(x,y)$ [8],

$$\Delta\Delta\chi(x,y) = 0, \tag{3}$$

in the infinite plane with traction-free boundary conditions on the crack surfaces

$$\sigma_{xn}(s) = \sigma_{yn}(s) = 0. \tag{4}$$

Here s is the arclength parametrization of the crack shape and $\sigma_{in}(s)$ denotes the stress acting in the ith direction on a segment whose outward normal is the normal to the crack face at s. The stress tensor field σ_{ij} is derivable from the Airy stress potential $\chi(x,y)$ according to

$$\sigma_{xx} = \frac{\partial^2\chi}{\partial y^2}, \quad \sigma_{xy} = -\frac{\partial^2\chi}{\partial x \partial y}, \quad \sigma_{yy} = \frac{\partial^2\chi}{\partial x^2}. \tag{5}$$

The relevant experimental configuration for our purpose is that of global mode I fracture in which a system containing *initially* a straight crack in the x direction, is subjected to a stress applied in the direction y, perpendicular to the crack. At infinity we write the boundary conditions

$$\sigma_{xx}(\infty) = 0, \quad \sigma_{yy}(\infty) = \sigma^{\infty}, \quad \sigma_{xy}(\infty) = 0, \tag{6}$$

where σ^{∞} is assumed to be constant.

Note that even though the initial configuration is that of a straight crack, with material disorder the crack might deviate from the straight path, attaining an arbitrary rough shape. Solving the bi-Laplace equation with boundary conditions on such an arbitrary boundary is quite a formidable task [9]. Recently, we have developed a general method of solution based on iterated conformal maps [10]. In this method, one starts with a crack for which the conformal map from the exterior of the unit circle to the exterior of the crack is known. For example, in our case we start with a long straight crack in the form of a mathematical branch cut, representing the common experimental practice of introducing the sample with a notch in order to localize the fracture process in a controlled way. We can then grow the crack by little steps in the desired directions, computing at all times the conformal map from the exterior of the unit circle to the exterior of the resulting crack. Having the conformal map makes the *exact* calculation of the stress field straightforward in principle [11] and highly affordable in practice. The details of the method and its machine implementations are described in full detail in Ref. [10].

B. Model *A*

1. Damage nucleation

We consider a crack evolving under quasistatic conditions by the nucleation and coalescence of damage ahead of the crack tip. These damage elements can be voids or microcracks. We focus on situations where only one damage element nucleates before the process of coalescence. This process is associated with a length scale ξ_c characteristic of the distance of the damage element from the tip. A plausible physical picture for such a process was proposed in Refs. [5,6]. The idea is to identify ξ_c with the size of the plastic zone that develops near the crack tip due to the large stresses concentrated there. More specifically, it was assumed that the material flows plastically such as to reduce the stress field near the crack tip to a level determined by the yield stress σ_Y. Mathematically, the statement is that the distortional energy $J_2 \equiv \frac{1}{2} s_{ij} s_{ij}$, with $s_{ij} \equiv \sigma_{ij} - \frac{1}{2}\mathrm{Tr}\,\boldsymbol{\sigma}\delta_{ij}$, satisfies the relation [12]

$$J_2 = \sigma_Y^2, \tag{7}$$

inside the plastic zone. Outside this region, the stress field behaves linear elastically. To find the outer boundary of the plastic zone, which has a characteristic length ξ_c, we use the iterated conformal mapping solution of the linear-elastic problem. We calculate the spatial curve for which Eq. (7) is satisfied when approaching the crack tip. This curve defines the elastic-plastic boundary. It was further shown [5,6] that the hydrostatic tension P, defined as

$$P \equiv \frac{1}{2}\mathrm{Tr}\,\boldsymbol{\sigma}, \tag{8}$$

attains a larger value near the elastic-plastic boundary than inside the plastic zone. Under the physically plausible assumption that damage will nucleate in regions where P exceeds some threshold value P_c, we expect damage to nucleate near this boundary. As was explained before, after damage nucleates it evolves such that it coalesces with the tip, generating a new plastic zone under the influence of the linear-elastic fields and so on. Note that in this physical interpretation the damage elements are plastic voids and the coalescence process is assumed plastic as well (for example, necking of the ligament between the crack tip and the void). In fact, as we are not resolving the processes by which the crack tip coalesces with the void ahead of it, we are using the nucleation site only as a pointer for the advance of the crack. Therefore, we are only interested in the roughness of the crack on scales larger than ξ_c.

2. Growth rule and disorder

Naturally, the precise location of the nucleating damage may be stochastic. To quantify this, assume that nucleation occurs only at locations $\mathbf{r}$ in which the hydrostatic tension P exceeds some threshold value P_c. Given the distribution $P(\mathbf{r})$ we consider a probability density function $f(P(\mathbf{r})-P_c)$. One has in mind an activation process for the nucleation of damage, and this activation is more efficient when $P(\mathbf{r})-P_c$ is large. The probability for activation vanishes for $P-P_c<0$. This activation may be due to stress corrosion in one case, or due to another mechanism in another case, but the important thing to note is that $P(\mathbf{r})$ is a long-ranged functional of the history of crack evolution, potentially leading to the long-range correlations implied by $\zeta>0.5$. The fact that damage nucleates depending on the stress field σ_{ij} through P without reference to any predetermined distribution of disorder implies that the model is characterized by *annealed disorder*. Note that the same formulation describes equally well a situation in which damage nucleates at points where the material is weak, if the *random* weak points are dense enough such that the typical scale d separating them is much smaller than ξ_c and that the distribution of nucleation thresholds is immaterial, characterized only by P_c. The relation $d \ll \xi_c$ allows us to take the continuum limit to define a probability distribution function. Model A was studied in Refs. [5,6]. In the absence of precise knowledge of the activation process we adopted reasonable probability distribution functions $f(P(\mathbf{r})-P_c)$ and demonstrated that the cracks generated by the model were self-affine with $\zeta=0.66\pm0.03$ *irrespective* of the specific form of $f(P(\mathbf{r})-P_c)$.

This model should be contrasted with the more common mathematical representation of stochastic growth models via a Langevin-type equation. In this case a *deterministic* equation is supplemented with an additive noise term whose statistics are independent of the deterministic part. In model A the randomness cannot be represented by an additive independent noise. We now turn to model B to test the influence of the type of randomness employed on the roughness of cracks.

C. Model *B*

In model B the crack is still assumed to propagate by the nucleation and coalescence of damage ahead of its tip. The linear-elastic stress fields are still calculated using the powerful method of iterated conformal mapping described in Sec. II A. The main difference between the two models stems from a different way of incorporating material disorder into the crack evolution process. In model B the disorder is assumed to be *quenched*, represented by an *a priori* random distribution of identical weak points. The random weak points have a prescribed density such that the average distance between them is d. Physically, the weak points can be realized by density fluctuations in an otherwise homogeneous material or by small particles that have a lower breaking threshold than the matrix in which they are embedded, but do not change significantly the elastic properties of the system. As in model A, the damage nucleation process near the crack tip is characterized by a length scale ξ_c. A second point of departure from model A is that in this model we assume $d \simeq \xi_c$. This relation can be realized in different physical situations. For example, ξ_c can still be identified (as in model A) with the linear dimension of the plastic zone, where the independent scale d just happens to be of the order of magnitude; in that case the damage elements can still be plastic voids. Alternatively, if plastic processes are not dominant, one could imagine the crack pinned to a weak point until a microcrack nucleates at another weak point to propagate the crack by coalescence. In this interpretation ξ_c is by definition of the order of d.

To complete the model we need a growth rule. As was mentioned before, the weak points are assumed identical in the sense that they have the same breaking threshold that is significantly smaller than the ordinary material points [13]. Since the disorder in this model is quenched, we can define a deterministic growth rule stating that the crack advances to the weak point where the hydrostatic tension P is maximal. Note that even though the weak points are spread randomly and independently of P, the selection of a weak point to be a pointer for the next crack growth depends crucially on its spatial proximity to the maximal hydrostatic tension P; the closest weak point to the maximal hydrostatic tension P is most likely to be chosen at each growth step. It is worthwhile mentioning that if one could fix ξ_c and decrease d such that $d/\xi_c \to 0$ (a limit that is not realized in our model where $d \simeq \xi_c$), one would obtain the *deterministic limit* of the model since the maximal hydrostatic tension P would almost inevitably coincide with a weak point and the crack would advance almost always to the point of maximal hydrostatic tension. Thus, the ratio d/ξ_c is a measure of the width of the statistical distribution in this model. Therefore, the discreteness of the disorder is an important factor, but cannot fully characterize the difference between the two models. To reiterate, the main differences between models A and B are as follows:

(1) In model B only the random weak points are potential sites for damage nucleation, while in model A every material point is in principle liable to damage nucleation, depending on the local hydrostatic tension $P(\mathbf{r})$.

(2) The growth rule in model B is deterministic, stating that at each step the weak point in which the local hydrostatic tension $P(\mathbf{r})$ is maximal will fail, while the growth rule in model A is stochastic, where the probability to nucleate damage depends on $P(\mathbf{r})-P_c$ through an activation process, where P_c is a material threshold.

(3) The intrinsic length scale ξ_c in model B is determined by the disorder length d, while the length scale ξ_c in model A is determined by the regularization of the linear-elastic singularity.

In the next section we analyze the new model and compare its results to the results of model A.

III. RESULTS AND DISCUSSION

The quenched disorder in model B is realized by generating random pairs (x_i, y_i) inside a large enough rectangle, such that each spatial point in the rectangle has the same probability to be occupied by a weak point. The number of random

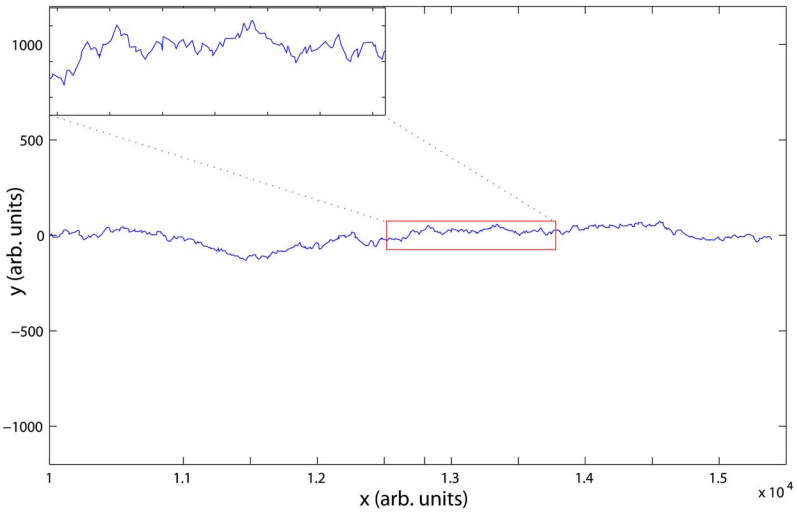

FIG. 1. (Color online) A typical crack of 500 growth steps in arbitrary units. Note the difference in scales between the ordinate and the abscissa. The inset shows a magnified segment of the crack corresponding to the rectangle. The overall scale of the ordinate of the inset plot is 100.

pairs is selected such that the average area per weak point is $\approx d^2$. The weak points are all assumed to have the same breaking threshold that is significantly lower than the breaking thresholds of ordinary material points. This ensures that the weak points act as pointers for the subsequent location of the crack tip at each step of the growth. We have verified that assigning a variable threshold picked from a Gaussian distribution whose width is comparable to the average (i.e., not too broad distributions) does not change the results presented below. It should be noted that extremely heterogenous materials characterized by threshold distributions with power-law tails are not considered here. Our picture applies to disordered materials that are characterized by a uniform spatial distribution of weak points with a *typical* breaking threshold. We have simulated the model and obtained several crack realizations, each of about 500 growth steps. An example of a resulting crack is shown in Fig. 1.

We have measured the roughness of the cracks in the model with both the variable bandwidth max-min method of Eq. (1) and the variable bandwidth rms method [14]. In order to avoid strong finite-size effects we have used the results of Ref. [14] to calibrate our exponents for the different measurement methods. This procedure was consistent in the sense that the variance in the results obtained by the different methods pointed to a single well-defined exponent according to the finite-size effects predicted in Ref. [14]. An example of a single roughness measurement using the variable bandwidth max-min method of Eq. (1), resulting in $\zeta=0.57$, is shown in Fig. 2. A similar measurement using the variable bandwidth rms method [14] yielded $\zeta=0.51$. For a crack length of ≈ 500 steps in this range of exponents, the first method is expected to overestimate the exponent, while the latter is expected to underestimate it [14]; therefore our estimation corresponds to the average of the two methods yielding $\zeta=0.54$. For the crack analyzed in Fig. 2, the disorder length d equals 15, therefore all the scales below d must be ignored and any relevant scaling behavior should be measured at higher scales. Indeed, the stable scaling range in the figure appears above the disorder length, while the scaling at lower scales is an artifact corresponding to the fact that the crack is advanced by straight lines between the selected weak points, contributing perfectly correlated small scale segments. Finally, we averaged over different realizations, obtaining $\zeta=0.53\pm0.03$.

This result indicates that the cracks in model *B* exhibit random roughness as the roughness exponent is not significantly different from the random-walk exponent $\zeta=0.5$. This result is qualitatively different from the results of model *A* in which $\zeta=0.66\pm0.03$. At this point we must conclude that even though the two models share many features and apparently one should not expect dramatically different scaling properties, the two models belong to different universality classes. Model *A* exhibits *correlated* roughening, while model *B* exhibits random roughening. We turn now to further clarifying the origin of the qualitatively different results.

A. Common (and nontrivial) properties of models *A* and *B*

The first thing to point out is that both models *A* and *B* deviate from many models common in the literature in a way

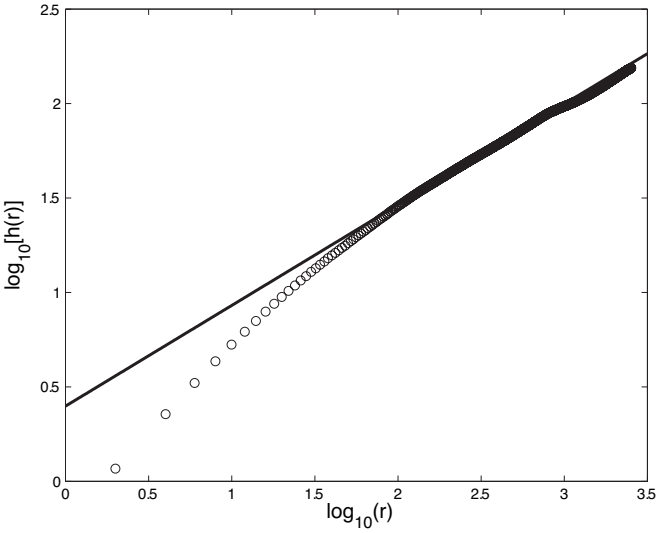

FIG. 2. A log-log plot of the height fluctuations $h(r)$ of Eq. (1) as a function of the scale r. The straight line corresponds to $\zeta=0.57$. A similar measurement using the variable bandwidth rms method [14] yielded $\zeta=0.51$, therefore our estimation in this case is $\zeta=0.54$ (see the text for more details).

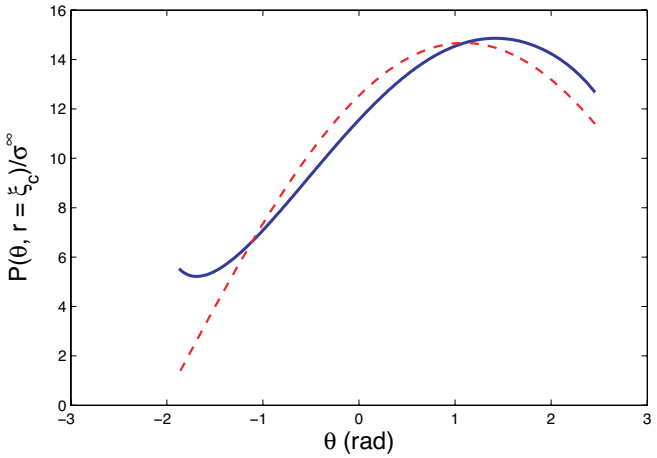

FIG. 3. (Color online) The hydrostatic tension P [see Eq. (8)], in units of σ^{∞}, as a function of θ (in radians) at a fixed radius $r=\xi_c$ (solid line) and a fit with $K_I=125$ (arbitrary units), $\frac{K_{II}}{K_I}=-0.51$ (dashed line). The present data was taken from a crack after 300 growth steps, but it is representative.

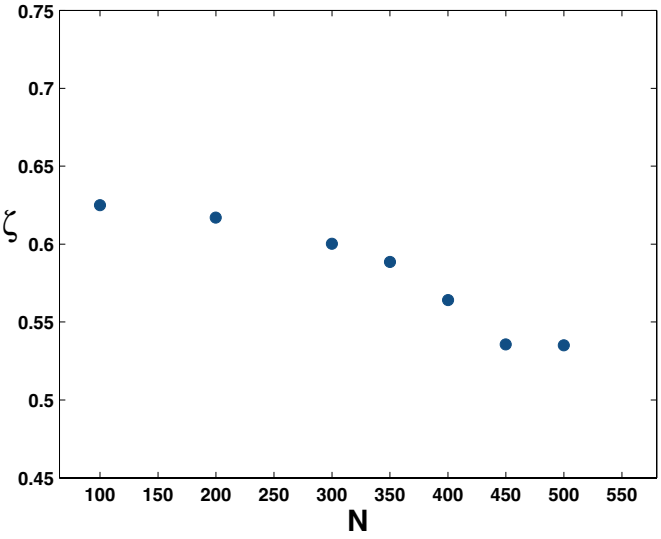

FIG. 4. (Color online) The average roughness exponent ζ as a function of the number of growth steps N for model B. The decrease towards a stationary state with $\zeta \approx 0.5$ is observed.

that might significantly affect the scaling properties. In ideal linear elasticity, the stress tensor field σ_{ij} attains the following asymptotic form approaching the crack tip:

$$\sigma_{ij}(r,\theta) = \frac{K_I}{\sqrt{2\pi r}}\Sigma_{ij}^{I}(\theta) + \frac{K_{II}}{\sqrt{2\pi r}}\Sigma_{ij}^{II}(\theta), \tag{9}$$

where (r,θ) is a polar coordinates system located at the crack tip, Σ^I and Σ^{II} are known universal functions, and K_I and K_{II} are the stress intensity factors corresponding to opening (mode I) and shearing (mode II) stresses [15]. Equation (9) describes well the stress fields on a scale r relative to the crack tip that is much smaller than any other length scale in the problem. The mode II stress intensity factor K_{II} is an important quantity for the understanding of the roughness of cracks since on the one hand it quantifies the near tip stress-field asymmetry, leading to crack deflection, while on the other hand it is *a long-range functional* of the crack shape $y(x)$, possibly generating long-range correlations. The calculation of $K_{II}\{y(x)\}$ is an extremely complicated mathematical problem and in fact can be tackled analytically only perturbatively. Usually, models include $K_{II}\{y(x)\}$ only to *linear order* in $y(x)$ [16], hoping that higher-order terms are not relevant for the scaling properties of cracks. It was already claimed in Ref. [17] that higher-order terms are crucial for the understanding of the roughness of cracks and might explain, at least partially, the failure of perturbative approaches to derive the experimental value of the roughness exponent [16]. The method of iterated conformal maps that was developed in Ref. [10] is nonperturbative in nature and therefore seems more suitable for the study of the development of crack roughness. Note that by specializing to first-order dynamics in $y(x)$, one essentially assumes that the local slopes are small. This assumption is clearly violated in our model (see, for example, the inset of Fig. 1).

In both models A and B the crack propagates via the nucleation and the coalescence of damage at a *finite* distance ξ_c ahead of its tip, essentially under the influence of a linear-elastic stress field. Naturally, we cannot expect Eq. (9) to be precise for r of the order of ξ_c. In particular, the hydrostatic tension $P(\mathbf{r})$ should be sensitive to significant corrections to the ideal behavior of Eq. (9). We can expect that the stress fields on a scale ξ_c away from the tip in both models is described by Eq. (9) with $K_I \gtrsim K_{II}$ *plus* additional, higher order in r, terms. Note that on this scale the crack is not straight anymore, but rather irregular. To verify this expectation we calculated the hydrostatic tension $P(r,\theta)$ on a constant arc a distance ξ_c from the tip and fitted it to the form

$$P(\theta) = \frac{K_I}{\sqrt{2\pi\xi_c}}\left[\cos\left(\frac{\theta}{2}\right) + \frac{K_{II}}{K_I}\sin\left(\frac{\theta}{2}\right)\right], \tag{10}$$

predicted by Eq. (9) [15]. The results support our expectation, showing that indeed $K_I \gtrsim K_{II}$ and demonstrating the existence of an additional contribution of 10–15 % from other nonuniversal terms at a distance ξ_c away from the tip for both models. An example of the result of such a fitting procedure is shown in Fig. 3.

The conclusion is that both models A and B, in contrast to traditional models, are deep in the nonlinear regime [in terms of the dependence of $K_{II}\{y(x)\}$ on $y(x)$] and moreover, one cannot neglect the influence of contributions on top of Eq. (9). Thus, not all the asymmetry near the crack tip is carried by $K_{II}\{y(x)\}$. We believe that this is an important aspect in the success of model A in reproducing a *correlated* roughening, quantitatively close to the experimental observations. It might also explain why models that used only K_{II} and to linear order in $y(x)$ achieved scaling exponents different from those observed in experiments [16,17].

On the other hand, this cannot be the only factor explaining the results of model A since this feature is common to model B, which fails to produce correlated roughening.

B. The difference between the models stems from the difference in randomness

We propose that the differences in randomness are responsible for the different universality classes of models *A* and *B*. Recall that the stochasticity in model *B* stems from the spatial quenched distribution of weak points whereas the growth rule itself is deterministic and that the quenched disorder length d is of the order of the nucleation length ξ_c. As a result, there are only a *few* weak points available for damage nucleation on a scale ξ_c. In this situation the crack "selects" a damage nucleation site out of a small number of possibilities and in fact there is a sizable probability of having a growth step chosen uncorrelated with the deterministic field P that carries information of the history of the evolution. We thus expect this randomization effect of uncorrelated growth steps to accumulate gradually and reduce the correlated roughening exponent observed in model *A*. The situation is fundamentally different in model *A* where the probability of having completely random growth steps is small. To support this explanation we have measured the roughness exponent ζ [see Eq. (2)] as a function of the crack length in terms of growth steps. In Fig. 4 we show the dependence of ζ on the number of growth steps.

It is observed that indeed the roughness exponent ζ decreases monotonically from $\zeta \approx 0.625$ to $\zeta \approx 0.53$, presumably approaching asymptotically $\zeta \approx 0.5$. This finding is consistent with the suggested explanation.

IV. SUMMARY

We have studied the role of disorder in generating a correlated roughening exponent in cracks of $1+1$ dimensions. The main conclusion is that adding additive material disorder to linear elasticity is not sufficient to generate correlated crack graphs with exponents larger than 0.5. This is due to the destructive events or uncorrelated steps which accumulate and gradually produce a random graph. The generation of correlated graphs ($\zeta > 0.5$) is due to the correlations between the deterministic field (the hydrostatic pressure) and the pdf carrying the randomness, like the annealed disorder of model *A*. We reiterate the result concerning the magnitude of the stress-intensity factors, and specifically K_{II}. The measurement of K_{II} and higher-order terms of the hydrostatic tension field tells us that linear approximations of K_{II}, or the principle of local symmetry, do not represent properly the stress field at the vicinity of ξ_c away from the rough crack tip. Therefore, one can view this feature as an additional test for models of crack growth, which produce the observed correlated roughness.

ACKNOWLEDGMENTS

This work has been supported in part by the Israel Science Foundation and by the German Israeli Foundation. I. Ben-Dayan thanks Eedo Mizrahi and Shani Sela for useful discussions. E. Bouchbinder is supported by the Horowitz Complexity Science Foundation.

[1] E. Bouchbinder, I. Procaccia, and S. Sela, Phys. Rev. Lett. **95**, 255503 (2005).
[2] J. Kertész, V. K. Horváth, and F. Weber, Fractals **1**, 67 (1993).
[3] T. Engøy, K. J. Måløy, A. Hansen, and S. Roux, Phys. Rev. Lett. **73**, 834 (1994).
[4] L. I. Salminen, M. J. Alava, and K. J. Niskanen, Eur. Phys. J. B **32**, 369 (2003).
[5] E. Bouchbinder, J. Mathiesen, and I. Procaccia, Phys. Rev. Lett. **92**, 245505 (2004).
[6] I. Afek, E. Bouchbinder, E. Katzav, J. Mathiesen, and I. Procaccia, Phys. Rev. E **71**, 066127 (2005).
[7] E. Bouchaud and F. Paun, Comput. Sci. Eng. **1**, 32 (1999).
[8] L. D. Landau and E. M. Lifshitz, *Theory of Elasticity*, 3rd ed. (Pergamon, London, 1986).
[9] D. Vandembroucq and S. Roux, Phys. Rev. E **55**, 6186 (1997).
[10] E. Bouchbinder, J. Mathiesen, and I. Procaccia, Phys. Rev. E **69**, 026127 (2004).
[11] N. I. Muskhelishvili, *Some Basic Problems of the Mathematical Theory of Elasticity* (Noordhoff, Groningen, 1953).
[12] J. Lubliner, *Plasticity Theory* (Macmillan, New York, 1990).
[13] This way of representing disorder is different, for example, from lattice models in which a threshold taken from an uncorrelated distribution is assigned to each lattice point. In that case the disorder is not introduced by the fluctuations in the locations of weak points (as in our model *B*), but by the fluctuations in the breaking thresholds. For more information on lattice models, see *Statistical Models for the Fracture of Disordered Media*, edited by H. J. Herrmann and S. Roux (North-Holland, Amsterdam, 1990).
[14] J. Schmittbuhl, J.-P. Vilotte, and S. Roux, Phys. Rev. E **51**, 131 (1995). See especially Figs. 8(a)–8(b).
[15] B. R. Lawn, *Fracture of Brittle Solids*, 2nd ed. (Cambridge University Press, Cambridge, England, 1998).
[16] S. Ramanathan, D. Ertas, and D. S. Fisher, Phys. Rev. Lett. **79**, 873 (1997).
[17] E. Bouchbinder, I. Procaccia, and S. Sela, J. Stat. Phys. (to be published).